NASA DEVELOP National Program
Alabama – Marshall

Fall 2021

Central America Disasters

Using Earth Observations to Map Flooding for Disaster Monitoring, Inform Potential Risk, and Prepare for Possible Response

DEVELOP Technical Report
Final – November 18th, 2021

Caroline Williams (Project Lead)
Lauren Carey
Maria De Los Santos
Deanna Fanelli
Payton Ireland

Advisors:
Kel Markert, NASA SERVIR Science Coordination Office (Science Advisor)
Eric Anderson, NASA SERVIR Science Coordination Office (Science Advisor)
Betzy Hernández, NASA SERVIR Science Coordination Office (Science Advisor)
Dr. Emil Cherrington, NASA SERVIR Science Coordination Office (Science Advisor)
Vanesa Martin, NASA SERVIR Science Coordination Office (Science Advisor)
Ronan Lucey, NASA Applied Sciences Disasters Program (Science Advisor)
Dr. Robert Griffin, University of Alabama Huntsville (Science Advisor)
Dr. Jeffrey Luvall, NASA Marshall Space Flight Center (Science Advisor)

1. Abstract

In November 2020, Hurricanes Eta and Iota hit Central America within weeks of each other, causing severe flooding, landslides, and widespread damage. NASA DEVELOP partnered with Comité Regional de Recursos Hidráulicos (CRRH), Centro de Coordinación para la Prevención de los Desastres en América Central y República Dominicana (CEPREDENAC), and Sistema de la Integración Centroamericana (SICA) to better understand how flooding throughout Central America has impacted and will continue to affect communities, focusing on sites in Guatemala, Honduras, El Salvador, Belize, Nicaragua, western Panama, and eastern Costa Rica from January 2015 to October 2021. The team utilized surface reflectance data from Landsat 7 Enhanced Thematic Mapper Plus (ETM+), Landsat 8 Operational Land Imager (OLI), Sentinel-2 MultiSpectral Instrument (MSI), Suomi National Polar-orbiting Partnership (NPP) Visible Infrared Imaging Radiometer Suite (VIIRS), and Terra Moderate Resolution Imaging Spectroradiometer (MODIS). This project also utilized backscatter data from Sentinel-1 C-band Synthetic Aperture Radar (C-SAR) and elevation data from the Shuttle Radar Topography Mission (SRTM). Incorporating these Earth observations in NASA SERVIR's Hydrologic Remote Sensing Analysis for Floods (HYDRAFloods) tool run on Google Earth Engine (GEE), the team produced historical surface water maps, a case study analysis of the two hurricanes, and a code tutorial. These results indicated that surface water increased in priority sites from 2015 to 2021, optical and SAR imagery detected similar flood patterns and extent after the hurricanes, and rainfall was concentrated on the east coast of the region. These products allow partners to make informed decisions around flooding preparation and disaster mitigation.

Key Terms

Central America, Hurricane Eta, Hurricane Iota, HYDRAFloods, flood mapping, disaster management, tropical cyclones

2. Introduction

2.1 Background Information

Just 13 days and 24 km apart, Hurricanes Eta and Iota devastated Central America in October and November 2020 (Shultz et al., 2021). No other two hurricanes have made landfall in Central America with such proximity and intensity (Shultz et al., 2021). The effects of these hurricanes included flooding, torrential downpours, property loss, power outages, displacement, and death (Shultz et al., 2021; Tellman et al., 2021). Floods are very costly natural disasters with estimated damages of up to $651 billion (USD) globally from 2000 to 2019 (Li et al., 2018; Tellman et al., 2021). Under most predicted climate change scenarios, floods and tropical cyclones are anticipated to increase in frequency as well as intensity (Hoque, et al., 2017; Tellman et al., 2021). As these flood impacts are anticipated to become progressively more severe, flood maps would greatly facilitate current decision-making processes and improve disaster monitoring and relief efforts (Li et al., 2018; Tellman et al., 2021).

Past research has used spaceborne sensors to detect the presence and extent of surface waters. Optical sensors that rely on sunlight to collect data have been the primary sensor used for surface water detection. However, these sensors cannot penetrate vegetation and cloud cover, making them inefficient in mapping flood events before meteorological conditions improve. In a 2018 study, Cian et al. used Synthetic Aperture Radar (SAR) to estimate flood depth and map flood extent. The key to their analysis was processing SAR data using the Normalized Difference Flood Index (NDFI) to highlight flooded areas, allowing them to easily separate flooded pixels from non-flooded pixels. The HYDrologic Remote Sensing Analysis for Floods (HYDRAFloods) is an open-source Python package built by SERVIR-Mekong on Google Earth Engine (GEE) with end-to-end processing that allows users to create their own high-quality surface water maps. Hietpas et al. (2021) used HYDRAFloods to understand the extent of flood risk in Fairfax County, Virginia. We used the Edge Otsu thresholding algorithm (Markert et al., 2020) to identify surface water extent in imagery captured before and after the hurricanes. Using HYDRAFloods, we leveraged inputs from multiple sensors in the creation of historical surface water maps. Remotely sensed satellite data can permit flood

mapping and aid policymakers and partner organizations in planning effective mitigation and disaster response management.

The study area of this project was Central America (Figure 1). The countries studied include Guatemala, Nicaragua, Honduras, Belize, and El Salvador along with portions of Costa Rica and Panama. These areas were identified as being the most impacted by Hurricanes Eta and Iota. We analyzed three time periods over the course of this project. For the Historical Surface Water Maps, the time period was January 2015 to October 2021, and the analysis focused on the whole study region. The Case Study Analysis focused on two weeks prior to Hurricane Eta, October 17th, 2020, through two weeks post Hurricane Iota on December 2nd, 2020, in Guatemala, Honduras, Nicaragua, and El Salvador. The Precipitation Analysis was conducted for the whole Central American region over a shorter time period from October 31st, 2020 to November 18th, 2020 as this is when most of the precipitation from Hurricanes Eta and Iota occurred.

Figure 1. A map showing the studied Central American countries of Guatemala, Nicaragua, Honduras, Belize, El Salvador, Costa Rica, and Panama.

2.2 Project Partners & Objectives

This project was conducted in collaboration with Sistema de la Integración Centroamericana (SICA), Comité Regional de Recursos Hidráulicos (CRRH), and Centro de Coordinación para la Prevención de los Desastres en América Central y República Dominicana (CEPREDENAC). SICA is an intergovernmental body that coordinates political and economic activities between member states. CRRH and CEPREDENAC are intergovernmental bodies under SICA focusing on water resource management and disaster response, respectively. While all partners possessed some knowledge of Earth observations, they were interested in

improving their capacity to use more Earth observations to better understand flooding throughout Central America and prepare effective responses. The primary benefits of this project include improving end users' ability to monitor surface water, understand flood risks, and create informed response efforts.

This project aimed to support partners' current disaster monitoring and response through remote sensing analysis and training materials. We created historical surface water maps and precipitation maps to identify possible areas of flood vulnerability. Our team carried out a case study of Hurricanes Eta and Iota using HYDRAFloods to demonstrate the potential of the tool for disaster analysis. Finally, we designed a coding tutorial for HYDRAFloods to enhance the partners' monitoring capacity.

3. Methodology

3.1 Data Acquisition

We retrieved data through Google Earth Engine provided by nine sources: NASA and US Geological Survey (USGS) Landsat imagery, European Space Agency (ESA) Sentinel imagery, NASA and National Oceanic and Atmospheric Administration (NOAA) Suomi National Polar Orbiting Partnership (NPP) Visible Infrared Imaging Radiometer Suite (VIIRS), NASA Terra Moderate Resolution Imaging Spectroradiometer (MODIS), the NASA Shuttle Radar Topography Mission (SRTM), the Climate Hazards Center's Infrared Precipitation with Station (CHIRPS) dataset, and the MERIT Hydro Global Hydrography Dataset by Yamazaki et al. (2019). We collected imagery from these varied platforms and sensors based on our study period for each analysis (Table 1). We chose a time period of October 17th, 2020 to December 2nd, 2020 for the Case Study Analysis to capture flooding before, during, and after the two events. Additionally, we focused this analysis on countries most impacted by the two hurricanes: Guatemala, Honduras, Nicaragua, and El Salvador. Data from the optical sensors were acquired for those dates and countries. Sentinel-1 C-band SAR data were retrieved for the timeline of the Historical Surface Water Analysis while the CHIRPS dataset was filtered to a smaller date range during Hurricanes Eta and Iota for the Precipitation Analysis.

Table 1
Earth observation platforms, sensors, and image capture dates used.

Platform / Sensor	**Parameters**	**Image Capture Dates**
Landsat 7 ETM+	Surface reflectance	10/17/2020 – 12/2/2020
Landsat 8 OLI	Surface reflectance	10/17/2020 – 12/2/2020
Sentinel-1 C-SAR	Backscatter	1/1/2015 – 10/22/2021
Sentinel-2 MSI	Surface reflectance	10/17/2020 – 12/2/2020
Suomi NPP VIIRS	Surface reflectance	10/17/2020 – 12/2/2020
Terra MODIS	Surface reflectance	10/17/2020 – 12/2/2020
SRTM	Elevation	10/17/2020 – 12/2/2020
CHIRPS	Precipitation	10/31/2020 – 11/18/2020
MERIT Hydro	Hydrography	10/17/2020 – 12/2/2020

3.2 Data Processing

3.2.1 SAR Processing

We processed Sentinel-1 C-band SAR imagery for both the Historical Surface Water Maps and the Case Study Analysis of Hurricanes Eta and Iota. Processing SAR imagery required four steps depicted in Figure 2. These included filtering by study area and period, applying a pseudo-terrain flattening correction, speckle filtering, and implementing an elevation mask for areas greater than 20 meters above the closest waterbody in the study area.

3.2.2 Optical Imagery Processing

We utilized several optical Earth observations, specifically Landsat 7 ETM+, Landsat 8 OLI, Sentinel-2 MSI, Suomi NPP VIIRS, and Terra MODIS, to examine flooding for the Case Study Analysis on Hurricanes Eta and Iota. Optical imagery processing was completed with the HYDRAFloods tool and the GEE Python API. The HYDRAFloods tool automatically applied a cloud masking algorithm. We then mosaicked the image collections for each satellite and sensor by day, resulting in a new image collection with one image per day. The images were mosaicked across three time periods: the before period (Oct. 17th, 2020 – Oct. 31st, 2020), the during period (Oct. 31st, 2020 – Nov. 18th, 2020) and the after period (Nov. 18th, 2020 – Dec. 2nd, 2020). Following this technique, we then reduced the image collection by the mode of each pixel based on the temporal resolution of the satellites and sensors that we utilized. Future users can adjust the reducer function to median or mean depending on the Earth observation used. This produced a final image for each of the three time periods across each satellite and sensor. Lastly, we calculated the Modified Normalized Difference Water Index (MNDWI) for these three time periods and for each satellite and sensor, which resulted in fifteen images (Equation 1) (Xu, 2006). These MNDWI outputs were used as the inputs to the data analysis.

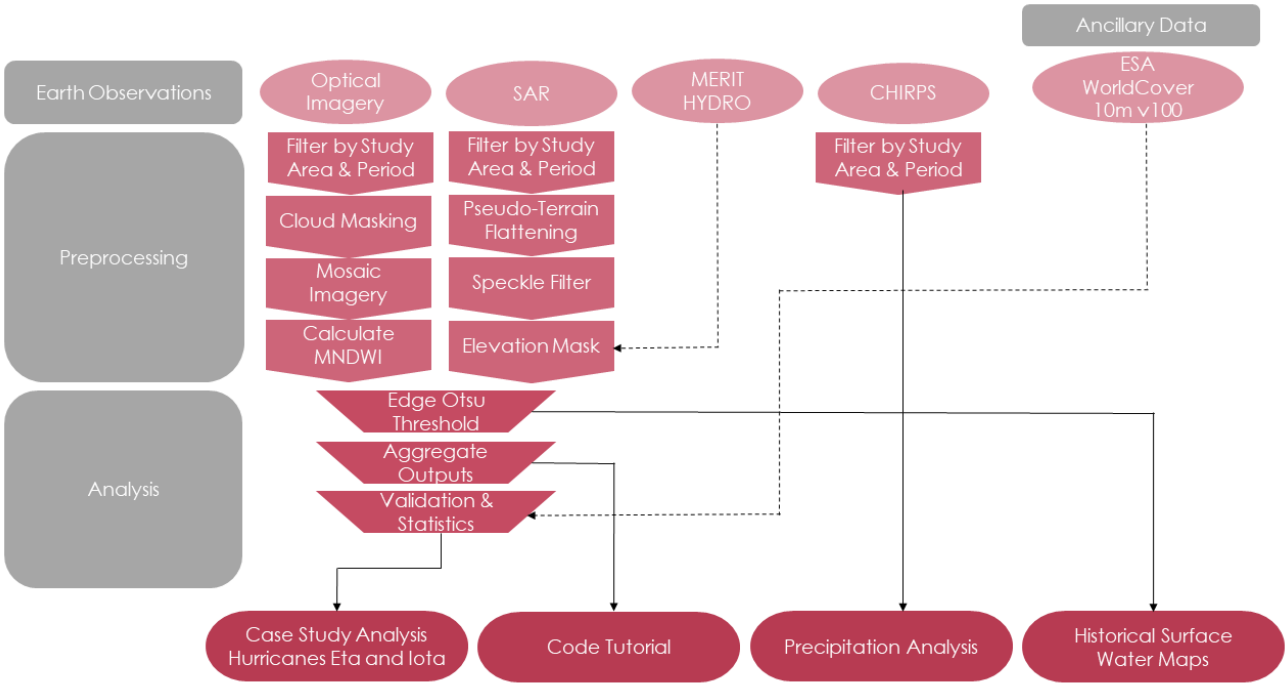

Figure 2. Case Study Analysis, Code Tutorial, Precipitation Analysis, and Historical Surface Water mapping workflow.

$$\text{MNDWI} = \frac{\text{GREEN - SWIR}}{\text{GREEN + SWIR}} \quad (1)$$

3.3 Data Analysis

3.3.1 Historical Surface Water Maps Analysis

The Edge Otsu thresholding algorithm extracts the edges of features in an image using a histogram-based approach (Canny, 1986; Donchyts et al., 2016; Markert et al., 2020; Otsu, 1979). Our team applied the Edge Otsu algorithm to previously generated surface water imagery to map historical surface water extent in 2015, 2016, 2017, 2018, 2020, and 2021. We examined the resulting maps in HYDRAFloods (v2021.10.11). The time and date of image acquisition can affect surface water classification, as seasonal variation can exaggerate surface water extent. As a comparison metric, our team used the Joint Research Center (JRC) Yearly Water Classification History (v1.3), a dataset containing maps of the location, distribution, and extent of surface

water from 1984 to 2020. Our team exported the six maps in the WGS 1984 geographic coordinate system and imported the GeoTIFF files into ArcGIS Pro 2.8. To understand how surface water has changed over time, we performed a change detection analysis by subtracting the surface water outputs between 2021 and 2015. We performed this step using the Raster Calculator tool in the spatial analysis toolbox in ArcGIS Pro 2.8. The resulting map can be found in section 4.1.1.

3.3.2 Case Study Analysis: Hurricanes Eta and Iota

3.3.2.1 Edge Otsu Thresholding

We employed two methodologies in examining Hurricanes Eta and Iota using the HYRDAFloods tool. The first analysis focused on the use of SAR imagery for flood mapping. The second methodology utilized optical imagery to extract flood information during and after the two hurricanes. Although the data processing differed between the SAR and optical imagery, we applied the same methods to extract flooding information. Using the HYDRAFloods tool, we implemented the Edge Otsu algorithm. In using the Edge Otsu function in HYDRAFloods, we defined the algorithm parameters depending on the satellite and sensor used. For imagery with a spatial resolution of 30 meters, we implemented an edge buffer of 300 meters. Meanwhile, for coarser imagery with a spatial resolution of 1000 meters, we defined the edge buffer as 1500 meters. More detail on the parameters used in the Edge Otsu algorithm in HYDRAFloods can be found in Table 2. The defined parameters include the scale, initial threshold, edge buffer, threshold no data, and whether to invert the result. For instance, the optical imagery required the invert parameter as we used MNDWI as an input to the algorithm. Parameters not detailed in Table 2 were left as the default values in HYDRAFloods. For each Earth observation product and time period, the algorithm generated a Boolean image in which pixels values of 1 indicated water and pixel values of 0 indicated areas of no water. We then extracted flood extent by masking permanent water over the results using the JRC Yearly Water Classification History dataset.

Table 2.

Parameters used in the Edge Otsu Threshold Algorithm in the HYDRAFloods tool to detect surface water extent. This was then subtracted from permanent water to extract flooding during and after Hurricanes Eta and Iota for the Case Study Analysis.

	Edge Otsu Threshold Algorithm Parameters				
Platform / Sensor	**Scale**	**Initial Threshold**	**Edge Buffer**	**Threshold No Data**	**Invert**
Landsat 7 ETM+	30	0	500	0	True
Landsat 8 OLI	30	0	300	0	True
Sentinel-1 C-SAR	180	-18	300	-0.2	False
Sentinel-2 MSI	30	0	300	0	True
Suomi NPP VIIRS	1000	0	1500	0	True
Terra MODIS	500	0	1000	0	True

3.3.2.2 Zonal Statistics

After classifying flooded areas, we performed a zonal statistics assessment to identify land cover types most impacted by the flooding during the two weeks after both hurricanes had passed. For the scale of the analysis, we obtained the Comisión Centroamericana de Ambiente y Desarrollo (CCAD) Watersheds (2008) dataset. We also utilized the European Space Agency (ESA) WorldCover 2020 10 m dataset using the GEE JavaScript API for our analysis. After acquiring the ESA dataset, we filtered to the pixel value for each land cover type, resulting in separate Boolean images. Next, we reprojected the flood image to correspond to the spatial resolution of the land cover image. Then we multiplied each land cover type by the flood image for each satellite and sensor to identify areas of flooding over the respective land cover type. Using the flooded land cover type outputs, we calculated total pixel area in square meters and calculated the sum of pixels by watershed. This was accomplished using the reduce regions function and the sum method. Finally, we

calculated the area in square kilometers and the percent of each land cover type's total area impacted by flooding following the two hurricanes.

3.3.3 Precipitation Analysis

The Climate Hazards Group InfraRed Precipitation with Station data (CHIRPS) was used to map daily and total event precipitation and to produce a daily precipitation graph for each country. In addition, we used GEE to generate two daily precipitation GIFs for Hurricane Eta and Iota. In total, four maps displayed total precipitation from October 31st to November 18th, 2020. We visualized each of these maps in GEE to see which areas received the most precipitation. Our team exported these four maps in the WGS 1984 geographic coordinate system and imported them to ArcGIS Pro 2.8 to display total event precipitation. Furthermore, we calculated the total precipitation per watershed using watershed shapefiles compiled by CCAD. The watershed analysis focused primarily on El Cajón Dam in Honduras. To calculate total precipitation at El Cajón Dam, our team used the Zonal Statistics tool in the spatial analyst toolbox in ArcGIS Pro 2.8. We created one daily precipitation graph per country using CHIRPS precipitation values acquired from GEE to quantify storm event precipitation further. Additionally, using GEE, our team created annual mean precipitation graphs for each country from 1999–2019 to further understand the trends in precipitation over Central America. More detailed methodology can be found in the Code Tutorial. Finally, the twenty-year period was chosen not to include precipitation due to Hurricane Mitch and Hurricane Eta and Iota.

4. Results & Discussion

4.1 Analysis of Results

4.1.1 Historical Surface Water Maps

Our team produced historical surface water maps from 2015 to 2021 to identify areas vulnerable to flooding. Figure 3 shows the results for 2021. The inset maps in each historical surface water map remained the same across the years, allowing for a visualization of the changes in surface water in priority sites determined by the partners and coastal areas. Differences were evident when comparing the surface water extent from 2015 to 2021 across the region. For example, Panama, Honduras, and Nicaragua displayed a visible increase in surface water extent across the study period.

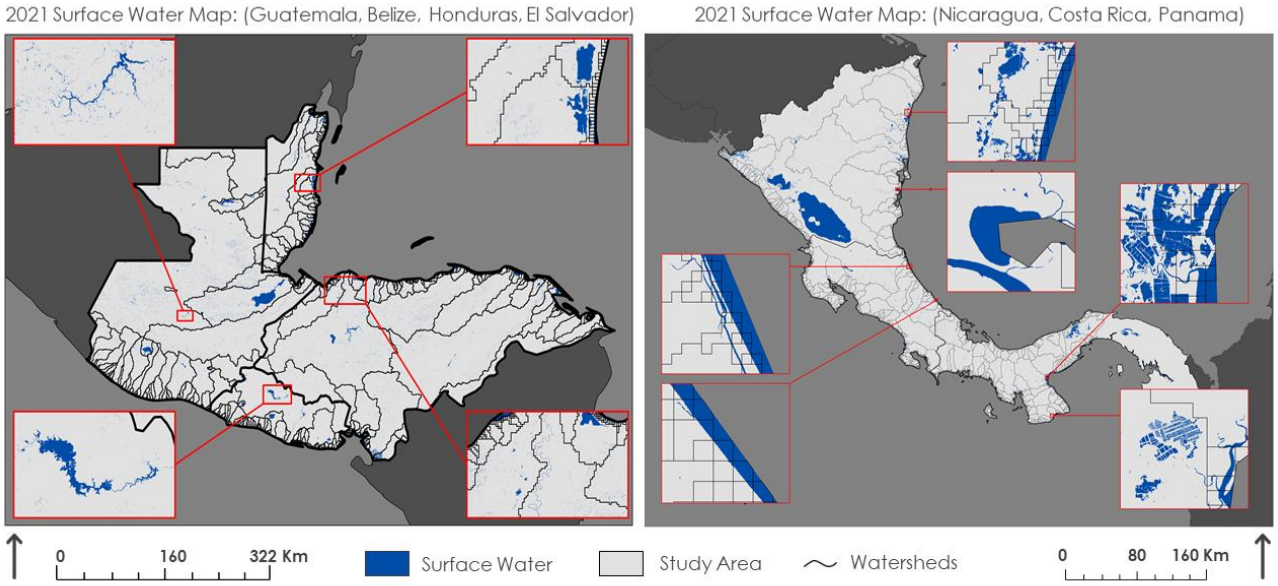

Figure 3. Surface water maps for 2021.

Figure 4, below, shows the results of the change detection analysis, allowing for a deeper understanding of how surface water extent has changed over the course of the study period. Purple areas indicate regions that have changed into surface water between 2015 and 2021. Orange areas denote regions that were classified as surface water in 2015 but are no longer classified as surface water as of 2021. Gray areas represent regions that have not changed across the study period.

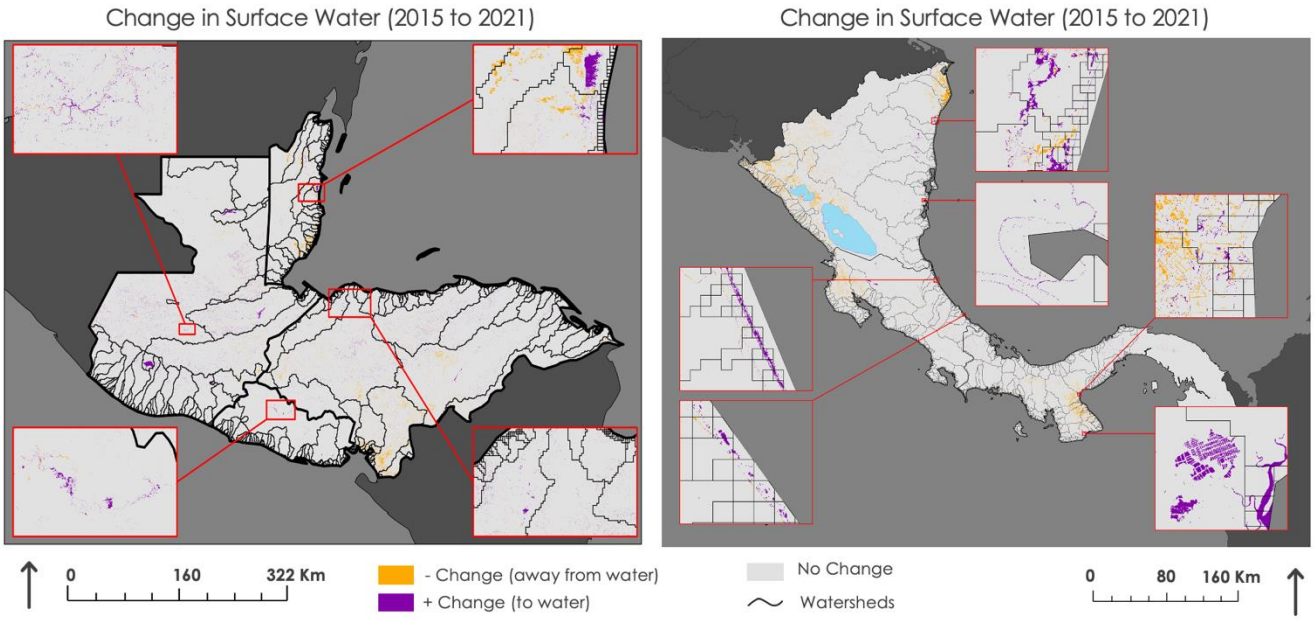

Figure 4. Surface water change detection maps (2015 to 2021).

All of the inset maps have some presence of purple pixels with varying degrees of intensity across sites. Panama, Nicaragua, and Costa Rica have a noticeable presence of purple pixels, indicating that these sites experienced increases in surface water extent from 2015 to 2021. The selected sites in Belize, Guatemala, El Salvador, and Honduras also have purple pixels. These results indicate that the priority areas and coastal regions highlighted in these maps did experience changes to surface water across the study period.

4.1.2 Case Study Maps: Hurricanes Eta and Iota

Though we examined Guatemala, Honduras, El Salvador, and Nicaragua, we present only the results for the Sula Valley below. The Sula Valley is a key agricultural region in northern Honduras traversed by the Ulua River and characterized by several important urban areas, including San Pedro Sula (Sanders et al., 2019). In examining the SAR flood maps, we also generated maps of flood extent at one week (Nov. 18th, 2020 – Nov. 25th, 2020), two weeks (Nov. 25th, 2020 – Dec. 2nd, 2020), and three weeks (Dec. 2nd, 2020 – Dec. 9th, 2020) after Hurricanes Eta and Iota in the Sula Valley, Honduras (Figure 5). We found that flooding persisted in this region even three weeks after the two hurricanes. Much of the cropland areas, identified by the ESA land cover dataset, were impacted by this long-lasting flooding.

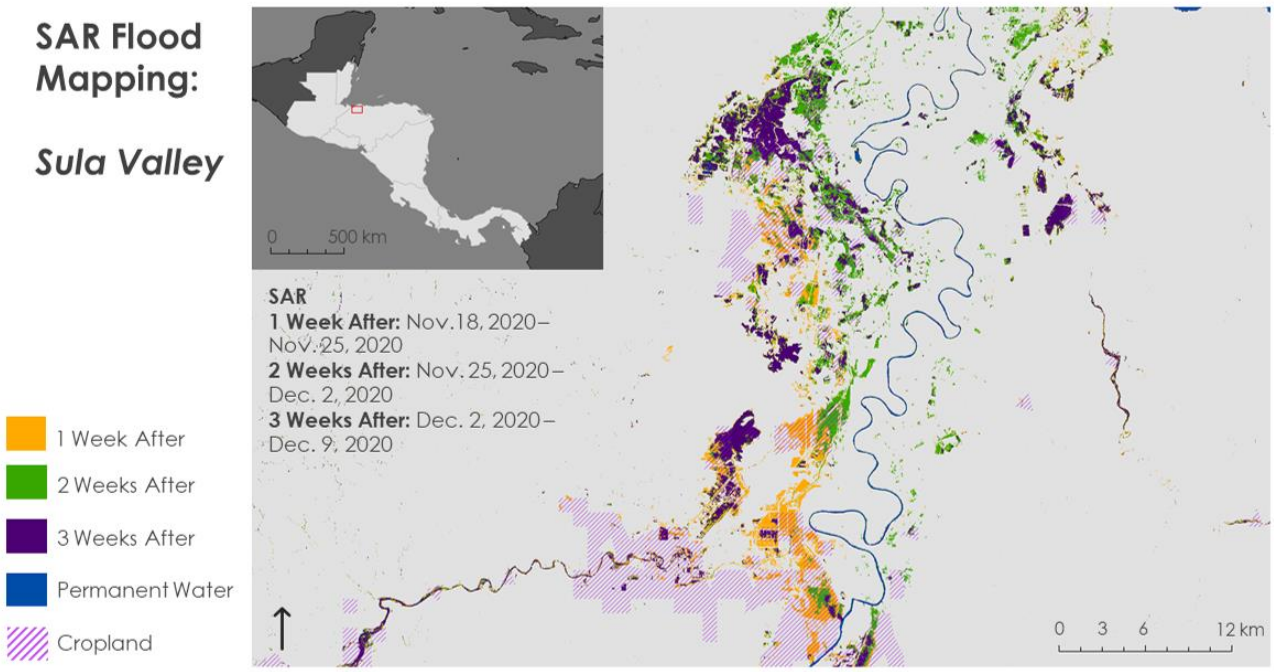

Figure 5. SAR flood map for Sula Valley, Honduras depicting flooding after Hurricanes Eta and Iota at one week, two weeks, and three weeks post-event.

We used Sentinel-1 C-Band SAR to visualize floods in the Sula Valley during and after Hurricanes Eta and Iota (Figure A1). Layering flood extent with the Cropland, Built-up, and Forest landcover classes highlighted potential impacts to the area. In addition to the SAR flood mapping results, we generated flood extent maps for Landsat 7 ETM+, Landsat 8 OLI, Sentinel-2 MSI, Suomi NPP VIIRS, and Terra MODIS. Figure A2 shows Terra MODIS flood extent maps during and after Hurricanes Eta and Iota in the Sula Valley. Flooding was extensive in both time periods with a minor decrease in extent in the after period. Although we generated flood extent images for the other optical satellites and sensors, only the Sentinel-2 MSI output had flood data for during and after in the Sula Valley. This speaks to a limitation in using optical imagery in flood detection analyses. Specifically, the other optical satellites and sensors used were not necessarily ineffective in extracting flood extent, but rather were limited due to cloud cover and low temporal resolution. Although limitations inhibited results for some time periods for optical satellites and sensors, we found that the optical image flood extent results agreed with the SAR flood extent maps.

Table 1 in Appendix A highlights twelve basins in seven watersheds where the priority sites identified by our partners were located. We conducted post-event zonal statistics at the watershed level between November 18th and December 2nd, 2020, on Built-up and Cropland because both landcover types are directly linked to human livelihood impacts. Overall, Landsat 7, Landsat 8, and NPP VIIRS detected the smallest areas of flooding in these two landcover classes while Sentinel-1, Sentinel-2, and Terra MODIS detected much larger areas. Sentinel-2 detected the highest total of flooded Cropland in the Río Salinas basin in the Río Usumacinta watershed (68.37 km^2), followed by Terra MODIS (45.15 km^2), NPP VIIRS (31.45 km^2), Sentinel-1 (28.34 km^2), and Landsat 7 (27.84 km^2). The Chamelecón and Ulua watersheds, located in the Sula Valley of Honduras, also experienced high flooding in cropland (Sentinel-1: 58.54 km^2 and 52.10 km^2; Sentinel-2: 24.26 km^2 and 23.62 km^2; Terra MODIS: 55.15 km^2 and 47.76 km^2; NPP VIIRS: 10.56 km^2 and 31.08 km^2; Landsat-8: 1.12 km^2 and 4.54 km^2; Landsat 7: No data and 0.18 km^2). In Built-up areas, the Ulua and Chamelecón watersheds again experienced the most flooding, as well as the Choluteca watershed on the Pacific coast. NPP VIIRS and Terra MODIS detected between 6.09 - 5.03 km^2 and 0.79 - 5.00 km^2 of flooding respectively for the Ulua, Chamelecón, and Choluteca watersheds. Landsat 7, Landsat 8, Sentinel-2, and Sentinel-1 detected little to no flooding in Built-up areas. Cloud coverage was persistent in our optical

imagery and SAR's limitations for flood detection in urban environments possibly contributed to its lower performance in Built-up areas.

4.1.3 Precipitation Maps

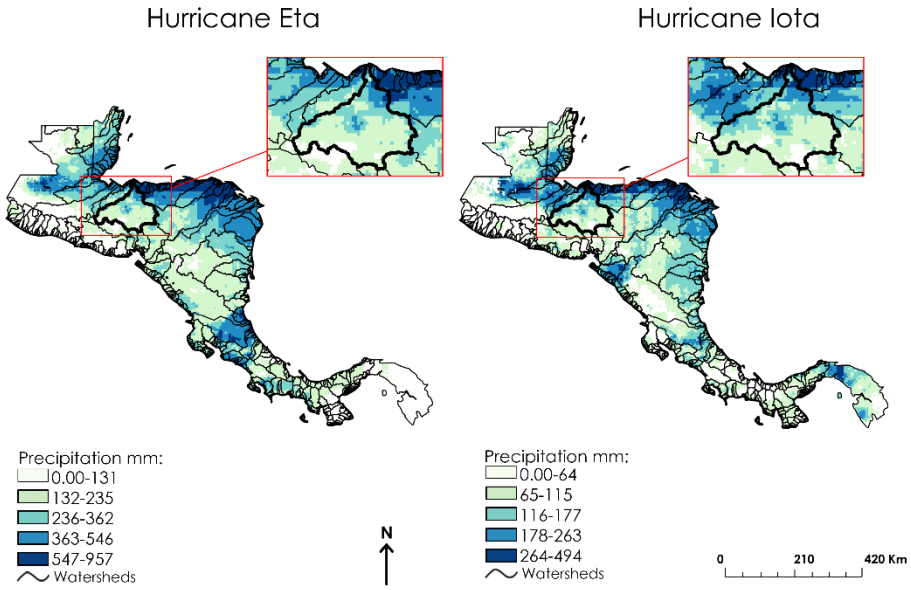

Figure 6. Total Event Precipitation Maps for Hurricane Eta and Hurricane Iota. Inset maps show El Cajón Dam (Honduras).

Our team produced total precipitation maps for Hurricane Eta and Hurricane Iota to identify areas that received the most precipitation over the course of the hurricanes (Figure 6). Most of the precipitation concentrated on the east side of Central America. Over thirteen days, Hurricane Eta deposited 957 mm (37 inches) of rain over Central America. Honduras received a total of 957 mm (37 inches) of rain, Guatemala received a total of 887 mm (35 inches), and Belize received a total of 545 mm (21 inches). Most of the rain during Hurricane Eta concentrated on the northern countries, with the exception of Costa Rica, which received 870 mm (34 inches) of rain.

Over five days, Hurricane Iota traversed some of the same areas as Hurricane Eta. The precipitation of Hurricane Iota began mainly in the southern countries of Nicaragua, Costa Rica, and Panama. Most of the heavy rains then migrated towards the northern countries of Honduras, Guatemala, and Belize. In total, Hurricane Iota deposited 494 mm (19 inches) of rain over Central America. Panama and Honduras received most of the rain. Panama received 494 mm (19 inches) of rain, and Honduras received 486 mm (17 inches).

Our team also produced a zonal statics table for El Cajón Dam (Honduras) (Table A2). El Cajón Dam, officially known as Central Hidroeléctrica Francisco Morazán, is a hydroelectric power plant in Western Honduras. This dam produces enough energy to power 189,000 homes (ENEE, 2009). The dam's watershed extends 21,963 km^2. During Hurricane Eta, this watershed received a total of 649 mm (25 inches) of precipitation. During Hurricane Iota, it received a total of 430 mm (17 inches) of rain. Overall, the watershed received 74% of the total precipitation of the storm events.

Figure A3 shows the daily precipitation per country during Hurricane Eta and Iota. During Hurricane Eta, all countries received maximum daily precipitation totals between October 31st and November 7th, with Honduras receiving 365 mm (14 inches) of rain on November 3rd and Guatemala receiving 678 mm (26 inches) of rain on November 5th. During Hurricane Iota, daily precipitation decreased for Guatemala and

Honduras and increased for Nicaragua, El Salvador, and Panama. Thus, Hurricane Iota deposited even more rain on countries that had already experienced high precipitation levels due to Hurricane Eta.

Figure 4 in Appendix A shows annual mean precipitation in the seven countries in the period 1999–2019. From highest to lowest, the 21-year averages are 2,920 mm (115 inches) for Costa Rica, 2,756 mm (108 inches) for Panama, 2,122 mm (86 inches) for Nicaragua, 1,963 mm (77 inches) for Belize,1,839 mm (72 inches) for Guatemala, 1,721 mm (68 inches) for El Salvador, and 1,623 mm (64 inches) for Honduras. The figure shows the region's variability in annual precipitation, a key factor as the region battles climate change.

4.2 Future Work

Our partner organizations have suggested additional studies that we were unable to conduct during our DEVELOP term. These included flood depth estimation maps for Hurricanes Eta and Iota as well as a rain threshold analysis. The use of HYDRAFloods in creating flood depth estimation maps from Hurricanes Eta and Iota would be advantageous to these organizations to see which areas were the most inundated with flooding as well as for how long. Our partner organizations also expressed interest in finding rain thresholds for flooding. Using the Historical Surface Water maps we created, a future project could study the areas we found to be vulnerable for a rain threshold analysis. Exploring data fusion methods such as logistic regression to combine SAR and optical flood maps for future analyses would also be useful, as this could lead to more accurate flood maps. Lastly, creating a Graphical User Interface (GUI) for HYDRAFloods specific to Central America would greatly benefit all of Central America. The GUI would allow anyone with access to the internet to view flood water maps of the area. These additional studies would be greatly beneficial to our partner organizations as well as to future DEVELOP participants.

5. Conclusions

Our project utilized NASA SERVIR's HYDRAFloods tool to assist partner organizations in Central America with improving their disaster monitoring and response efforts. We used SAR imagery to create historical surface water maps for the region from 2015 to 2021, highlighting coastal areas and priority areas chosen by the partners. We also used a combination of SAR and optical imagery to conduct a case study analysis of the impacts of Hurricanes Eta and Iota on the region. Further, our team processed CHIRPS data in GEE to perform a precipitation analysis of both hurricanes. All of these analyses are explained in a code tutorial, equipping partners with the ability to apply these techniques and processes to monitor future disasters and flooding events. Our results for the surface water analysis indicate that the areas displayed in inset maps did experience changes in surface water across the study period, with all of the highlighted areas displaying increases in surface water extent. The changes in surface water extent could indicate that these areas are prone to flooding. The results of the case study analysis demonstrate that using a combination of SAR and optical imagery is effective in detecting flooding extent after a hurricane. We saw agreement in flooding patterns across several different satellites and sensors, showing that the various Earth observations detected similar flood coverage. Finally, the precipitation analysis demonstrated that Hurricanes Eta and Iota deposited excessive rainfall across Central America with the eastern coasts receiving the most. Some areas experienced as much as 1,400 millimeters of rain. Ultimately, these results and the code tutorial will improve our partners' capacity to replicate these analyses in future flooding events.

6. Acknowledgments

We, the Central America Disasters team, would like to thank our science advisor at the Marshall Space Flight Center, Dr. Jeffrey Luvall, and the team at the NASA SERVIR Science Coordination Office: Kel Market, Eric Anderson, Betzy Hernández, Emil Cherrington, and Vanesa Martin. We are also grateful for the support of Ronan Lucey from the NASA Applied Sciences Disasters Program, Robert Griffin from University of Alabama Huntsville, and Paxton LaJoie, our NASA DEVELOP Fellow. Additionally, we would like to acknowledge our partners and thank them for their collaboration throughout this project: Berta Olmedo Vernaza from CRRH, Marcelo Oyuela from CEPREDENAC, and Jorge Cabrera from SICA.

This material contains modified Copernicus Sentinel data (2015 – 2021), processed by ESA.

Any opinions, findings, and conclusions or recommendations expressed in this material are those of the author(s) and do not necessarily reflect the views of the National Aeronautics and Space Administration. This material is based upon work supported by NASA through contract NNL16AA05C.

7. Glossary

CEPREDENAC – Centro de Coordinacion Para la Prevencion de los Desastres en America Central y Republica Dominicana – Partner organization
CHIRPS – Climate Hazards center InfraRed Precipitation with Station data – Rainfall data set
CRRH – Comite Regional de Recursos Hidraulicos – Partner organization
Earth observations – Satellites and sensors that remotely observe the Earth and extract information
ESA – European Space Agency
ETM+ – Enhanced Thematic Mapper Plus – Sensor aboard the Landsat 7 satellite
GEE – Google Earth Engine
HYDRAFloods – Hydrologic Remote Sensing Analysis for Floods – A program used to process satellite imagery to produce flood maps
MODIS – Moderate Resolution Imaging Spectroradiometer – Sensor aboard the Terra and Aqua satellites
MNDWI – Modified Normalized Difference Water Index
NDVI – Normalized Difference Vegetation Index
MSI – Multi-Spectral Instrument – Sensor aboard the Sentinel-2 satellite
NOAA – National Oceanic and Atmospheric Administration
NPP – National Polar-orbiting Partnership – NOAA weather satellite
OLI – Operational Land Imager – Sensor aboard the Landsat 8 satellite
SAR – Synthetic Aperture Radar – Sensor aboard the Sentinel-1 satellite
SICA – Sistema de la Integracion Centroamericana – Partner organization
SRTM – Shuttle Radar Topography Mission – Elevation dataset
USGS – United States Geological Survey
VIIRS – Visible Infrared Imaging Radiometer Suite – Sensor aboard the Suomi NPP satellite

8. References

Canny, J. (1986). A computational approach to edge detection. *IEEE Transactions on Pattern Analysis and Machine Intelligence*, *PAMI-8*(6), 679–698. https://doi.org/10.1109/TPAMI.1986.4767851

Cian, F., Marconcini, M., Ceccato, P., & Giupponi, C. (2018). Flood depth estimation by means of high-resolution SAR images and lidar data. *Natural Hazards and Earth System Sciences*, *18*, 3063–3084. https://doi.org/10.5194/nhess-18-3063-2018

Climate Hazards Center, University of California Santa Barbara and United States Geological Survey (USGS). *CHIRPS Daily: Climate Hazards Group InfraRed Precipitation with Station Data (Version 2.0 Final).* https://doi.org/10.1038/sdata.2015.66

DeVries, B., Huang, C., Armston, J., Huang, W., Jones, J. W., & Lang, M. W. (2020). Rapid and robust monitoring of flood events using Sentinel-1 and Landsat data on the Google Earth Engine. *Remote Sensing of Environment*, *240*, Article 111664. https://doi.org/10.1016/j.rse.2020.111664

Donchyts, G., Schellekens, J., Winsemius, H., Eisemann, E., & Van de Giesen, N. (2016). A 30 m resolution surface water mask including estimation of positional and thematic differences using Landsat 8,

SRTM and OpenStreetMap: A case study in the Murray-Darling Basin, Australia. *Remote Sensing*, *8*(5), Article 386. https://doi.org/10.3390/rs8050386

European Space Agency. Copernicus Open Access Hub (2015-2021). Sentinel 1 C-Synthetic Aperture Radar [Data set]. https://sentinels.copernicus.eu/web/sentinel/user-guides/sentinel-1-sar

European Space Agency. Copernicus Open Access Hub (2020). *Sentinel 2A and 2B Multispectral Instrument (MSI)* [Data set]. https://sentinels.copernicus.eu/web/sentinel/technical-guides/sentinel-2-msi

Empresa Nacional de Energía Eléctrica (ENEE). (2009). *Represa Hidroeléctrica Francisco Morazán "El Cajón."* https://web.archive.org/web/20090916221811/http://www.enee.hn/represaFM.htm

Hietpas, K., Ochoa-Madrid, E., Williams, E., & Spencer, O. (2021). *Fairfax Water Resources: Estimating urban flood susceptibility, historical flooding extent, and land cover change in Fairfax County, Virginia to aid in flood mitigation planning.* [Unpublished manuscript] NASA DEVELOP National Program, Virginia – Langley.

Hoque, M. A.-A., Phinn, S., & Roelfsema, C. (2017). A systematic review of tropical cyclone disaster management research using remote sensing and spatial analysis. *Ocean & Coastal Management*, *146*, 109–120. https://doi.org/10.1016/j.ocecoaman.2017.07.001

Irwin, K., Beaulne, D., Braun, A., & Fotopoulos, G. (2017). Fusion of SAR, optical imagery, and airborne LiDAR for surface water detection. *Remote Sensing*, *9*(9), Article 890. MDPI AG. http://dx.doi.org/10.3390/rs9090890

Li, S., Sun, D., Goldberg, M. D., Sjoberg, B., Santek, D., Hoffman, J. P., DeWeese, M., Restrepo, P., Lindsey, S., & Holloway, E. (2018). Automatic near real-time flood detection using Suomi-NPP/VIIRS data. *Remote Sensing of Environment*, *204*, 672–689. https://doi.org/10.1016/j.rse.2017.09.032

Markert, K. N., Markert, A. M., Mayer, T., Nauman, C., Haag, A., Poortinga, A., Bhandari, B., Thwal, N. S., Kunlamai, T., Chishtie, F., Kwant, M., Phongsapan, K., Clinton, N., Towashiraporn, P., & Saah, D. (2020). Comparing Sentinel-1 surface water mapping algorithms and radiometric terrain correction processing in Southeast Asia utilizing Google Earth Engine. *Remote Sensing*, *12*(15), Article 2469. https://doi.org/10.3390/rs12152469

NASA JPL (2013). *NASA Shuttle Radar Topography Mission Global 3 arc second* [Data set]. NASA EOSDIS Land Processes DAAC. https://doi.org/10.5067/MEaSUREs/SRTM/SRTMGL3.003

Otsu, N. (1979). A threshold selection method from gray-level histograms. *IEEE Transactions on Systems, Man, and Cybernetics*, *9*(1), 62-66. https://doi.org/10.1109/TSMC.1979.4310076

Sanders, A., Thomas, T. S., Rios, A., & Dunston, S. (2019). Climate change, agriculture, and adaptation options for Honduras. *International Food Policy Research Institute (IFPRI)*, Discussion Paper 01827. https://doi.org/10.2499/p15738coll2.133215

Shultz, J. M., Berg, R. C., Kossin, J. P., Burkle Jr, F., Maggioni, A., Pinilla Escobar, V. A., Castillo, M. N.,

Espinel, Z., & Galea, S. (2021). Convergence of climate-driven hurricanes and COVID-19: The impact of 2020 hurricanes Eta and Iota on Nicaragua. *The Journal of Climate Change and Health*, *3*, Article 100019. https://doi.org/10.1016/j.joclim.2021.100019

Tellman, B., Sullivan, J. A., Kuhn, C., Kettner, A. J., Doyle, C. S., Brakenridge, G. R., Erickson, T. A., & Slayback, D. A. (2021). Satellite imaging reveals increased proportion of population exposed to floods. *Nature*, *596*(7870), 80–86. https://doi.org/10.1038/s41586-021-03695-w

US Geological Survey Earth Resources Observation and Science Center (2020). Landsat 7 ETM+ Level-2 Data Products – Surface Reflectance [Data set]. US Geological Survey. https://doi.org/10.5066/F7Q52MNK

U.S. Geological Survey Earth Resources Observations and Science Center. (2020). *Landsat OLI/TIRS Level-2 Surface Reflectanc*e [Data set]. U.S. Geological Survey. https://doi.org/10.5066/f78s4mzj

Vermote, E. & Wolfe, R. (2015). *MOD09GA MODIS/Terra Surface Reflectance Daily L2G Global 1kmand 500m SIN Grid V006* [Data set]. NASA EOSDIS Land Processes DAAC. https://doi.org/10.5067/MODIS/MOD09GA.006

Vermote, E., Franch, B., & Claverie, M. (2020). *VIIRS/NPP Surface Reflectance Daily L2G Global 1km and 500m SIN Grid V001* [Data set]. NASA EOSDIS Land Processes DAAC. https://doi.org/10.5067/VIIRS/VNP09GA.001

*Landsat OLI/TIRS Level-2 Surface Reflectanc*e [Data set]. U.S. Geological Survey. https://doi.org/10.5066/f78s4mzj

Xu, H. (2006). Modification of normalized difference water index (NDWI) to enhance open water features in remotely sensed imagery. *International Journal of Remote Sensing*, *27*(14), 3025–3033. https://doi.org/10.1080/01431160600589179

Yamazaki, D., Ikeshima, D., Sosa, J., Bates, P.D., Allen, G.H., & Pavelsky, T.M. (2019) MERIT Hydro: A high-resolution global hydrography map based on latest topography datasets. *Water Resources Research*, *55*(6), 5053–5073. https://doi.org/10.1029/2019WR024873

9. Appendices

Appendix A

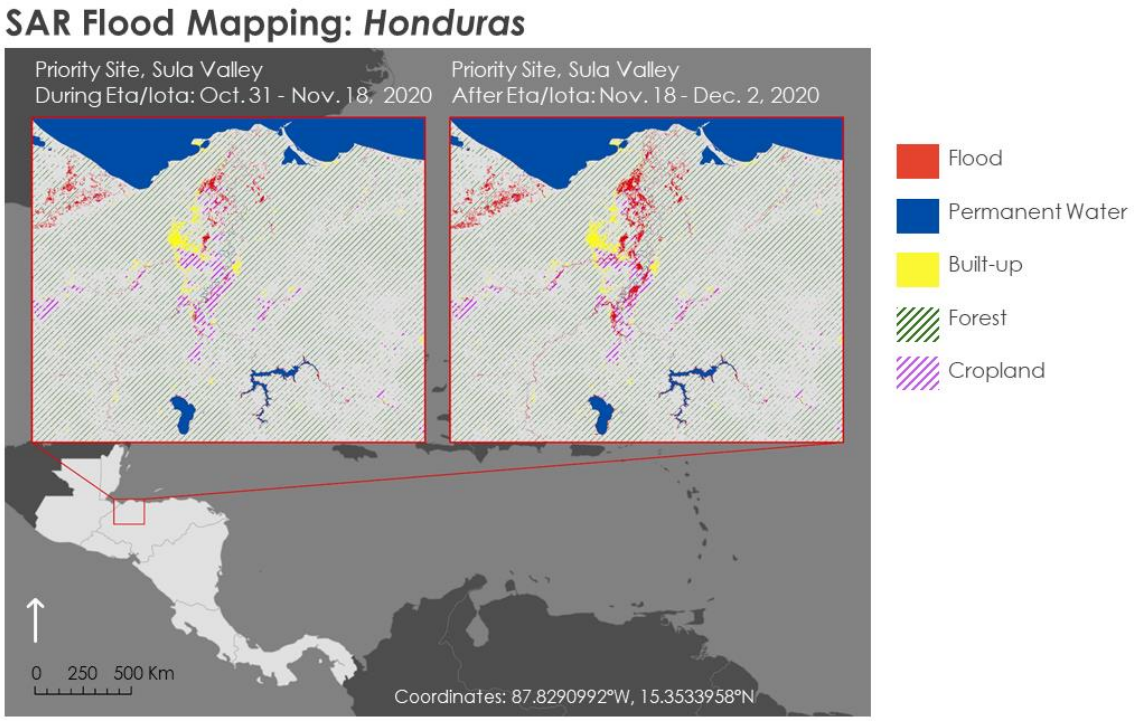

Figure A1. SAR flood map for Sula Valley, Honduras depicting flood during and after Hurricane Eta and Iota.

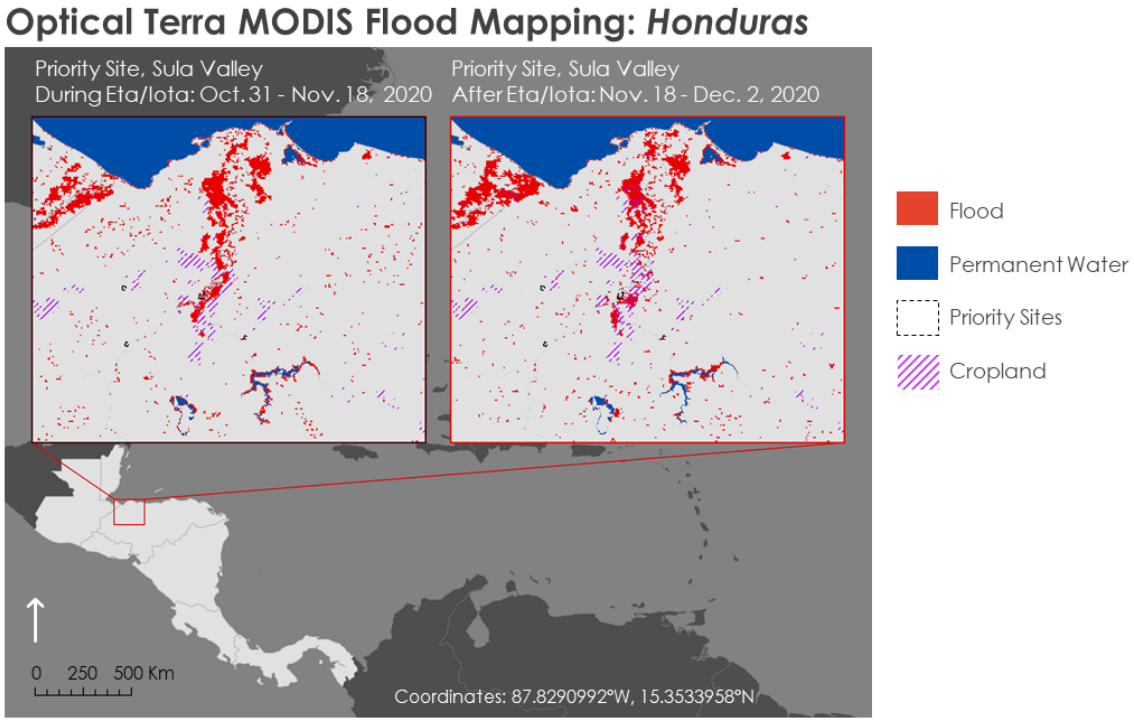

Figure A2. Optical flood map for Sula Valley, Honduras depicting flood during and after Hurricane Eta and Iota. This map shows Terra MODIS results.

Table A1.

Built-up and Cropland Flooded by Selected Watersheds, Nov. 18 – Dec. 2, 2020 (Cont. next page).

WATERSHED	BASIN ID		LANDSAT 7		LANDSAT 8		TERRA MODIS	
			Built-up	Cropland	Built-up	Cropland	Built-up	Cropland
Chamalecon *(Honduras)*	123440	Area km²	No data	No data	0.00	1.12	4.03	55.15
		%	No data	No data	0.00	0.57	3.09	27.89
Choluteca *(Honduras)*	131576	Area km²	0.12	1.38	0.10	0.12	0.72	3.54
		%	0.10	0.38	0.09	0.03	0.57	0.99
Lean *(Honduras)*	124178	Area km²	No data	No data	No data	No data	0.18	4.95
		%	No data	No data	No data	No data	4.83	63.03
	124438	Area km²	No data	No data	0.00	0.11	0.05	0.02
		%	No data	No data	0.01	1.43	0.80	0.20
Ulua *(Honduras)*	123189	Area km²	0.22	0.18	0.06	4.54	5.00	47.76
		%	0.12	0.04	0.04	0.96	2.76	10.10
Rio Dulce *(Guatemala)*	124633 *(Rio Cahabon)*	Area km²	0.01	0.03	0.00	0.14	0.20	2.51
		%	0.07	0.30	0.00	1.49	1.16	26.25
Rio Motagua *(Guatemala / Honduras)*	125504 *(Rio Motagua)*	Area km²	0.40	0.67	0.26	6.41	0.86	34.46
		%	0.15	0.15	0.10	1.40	0.33	7.51
	125504 *(Rio Grande de Zacapa)*	Area km²	0.04	0.51	0.02	0.25	0.09	0.85
		%	0.12	0.74	0.06	0.36	0.25	1.24
Rio Usumacinta *(Guatemala)*	99565 *(Rio Ixcan)*	Area km²	0.00	0.41	0.00	0.06	0.01	0.00
		%	0.01	4.10	0.00	0.63	0.09	0.00
	99565 *(Rio Xaclbal)*	Area km²	0.00	0.19	No data	No data	0.01	0.00
		%	0.05	2.23	No data	No data	0.30	0.06
	99565 *(Rio Salinas)*	Area km²	0.13	27.84	0.00	0.00	0.43	45.15
		%	0.20	8.50	0.00	0.00	0.66	13.79
	99565 *Rio La Pasion*	Area km²	0.07	2.42	0.00	0.01	0.05	1.97
		%	0.22	2.83	0.00	0.01	0.16	2.30

Table A1 (Cont.).

Continued. Built-up and Cropland Flooded by Selected Watersheds, Nov. 18 – Dec. 2, 2020

WATERSHED	BASIN ID		NPP VIIRS		SENTINEL-1		SENTINEL-2	
			Built-up	Cropland	Built-up	Cropland	Built-up	Cropland
Chamalecon *(Honduras)*	123440	Area km²	5.92	10.56	0.81	58.54	0.89	24.26
		%	4.53	5.34	0.62	29.61	0.68	12.27
Choluteca *(Honduras)*	131576	Area km²	5.03	3.43	0.12	2.11	0.05	0.47
		%	3.95	0.96	0.10	0.59	0.59	0.52
Lean *(Honduras)*	124178	Area km²	0.38	1.08	0.00	5.45	0.01	1.31
		%	10.37	13.79	0.02	69.42	0.32	16.63
	124438	Area km²	0.48	0.29	0.00	1.18	0.01	1.12
		%	7.82	3.67	0.08	14.89	0.10	14.18
Ulua *(Honduras)*	123189	Area km²	6.09	31.08	0.52	52.10	0.53	23.62
		%	3.36	6.57	0.29	11.02	0.29	5.00
Rio Dulce *(Guatemala)*	124633 *(Rio Cahabon)*	Area km²	0.19	0.04	0.01	0.78	0.17	2.44
		%	1.13	0.39	0.07	8.20	0.98	25.55
Rio Motagua *(Guatemala / Honduras)*	125504 *(Rio Motagua)*	Area km²	3.12	11.75	0.21	32.09	6.82	35.68
		%	1.20	2.56	0.08	6.99	2.61	7.77
	125504 *(Rio Grande de Zacapa)*	Area km²	0.24	2.12	0.05	2.15	No data	No data
		%	0.65	3.07	0.13	3.12	No data	No data
Rio Usumacinta *(Guatemala)*	99565 *(Rio Ixcan)*	Area km²	0.02	0.00	0.01	1.51	0.00	0.85
		%	0.18	0.00	0.13	15.00	0.04	8.42
	99565 *(Rio Xaclbal)*	Area km²	0.04	0.14	0.00	1.41	0.02	0.31
		%	0.82	1.66	0.00	16.91	0.55	3.68
	99565 *(Rio Salinas)*	Area km²	0.80	31.46	0.08	28.34	0.43	68.37
		%	1.25	9.61	0.12	8.66	0.67	20.88
	99565 *Rio La Pasion*	Area km²	0.75	0.68	0.09	3.41	0.11	3.28
		%	2.31	0.79	0.29	3.99	0.33	3.83

Table A1 (Cont.).

Continued. Built-up and Cropland Flooded by Selected Watersheds, Nov. 18 – Dec. 2, 2020

WATERSHED	BASIN ID		SUMMARY			
			Built-up	Min	Max	Mean
Chamalecon *(Honduras)*	123440	Area km²	No data	0.00	58.54	16.13
		%	No data	0.00	29.61	8.46
Choluteca *(Honduras)*	131576	Area km²	0.12	0.05	5.03	1.43
		%	0.10	0.03	3.95	0.74
Lean *(Honduras)*	124178	Area km²	No data	0.00	5.45	1.67
		%	No data	0.02	69.42	22.30
	124438	Area km²	No data	0.00	1.18	0.33
		%	No data	0.01	14.89	4.32
Ulua *(Honduras)*	123189	Area km²	0.22	0.06	52.10	14.31
		%	0.12	0.04	11.02	3.38
Rio Dulce *(Guatemala)*	124633 *(Rio Cahabon)*	Area km²	0.01	0.00	2.51	0.54
		%	0.07	0.00	26.25	5.47
Rio Motagua *(Guatemala / Honduras)*	125504 *(Rio Motagua)*	Area km²	0.40	0.21	35.68	11.06
		%	0.15	0.08	7.77	2.57
	125504 *(Rio Grande de Zacapa)*	Area km²	0.04	0.02	2.15	0.63
		%	0.12	0.06	3.12	0.97
Rio Usumacinta *(Guatemala)*	99565 *(Rio Ixcan)*	Area km²	0.00	0.00	1.51	0.24
		%	0.01	0.00	15.00	2.38
	99565 *(Rio Xaclbal)*	Area km²	0.00	0.00	1.41	0.21
		%	0.05	0.00	16.91	2.62
	99565 *(Rio Salinas)*	Area km²	0.13	0.00	68.37	16.92
		%	0.20	0.00	20.88	5.36
	99565 *Rio La Pasion*	Area km²	0.07	0.00	3.41	1.07
		%	0.22	0.00	3.99	1.42

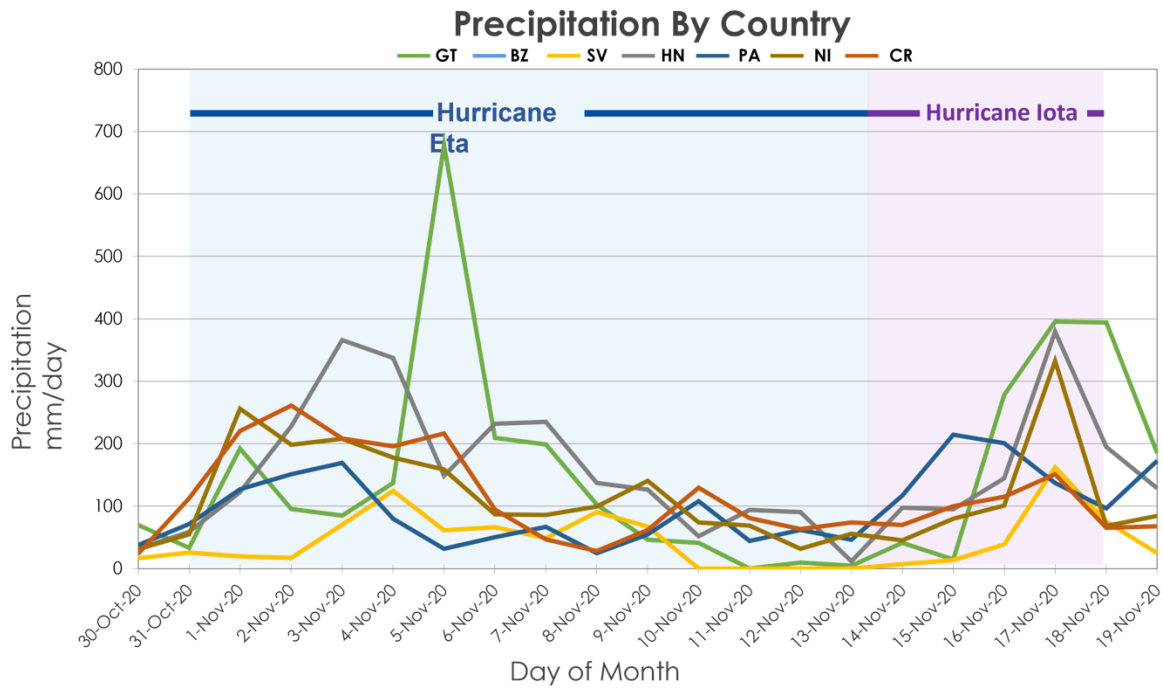

Figure A3. Hurricane Eta and Hurricane Iota Daily Precipitation per Country.

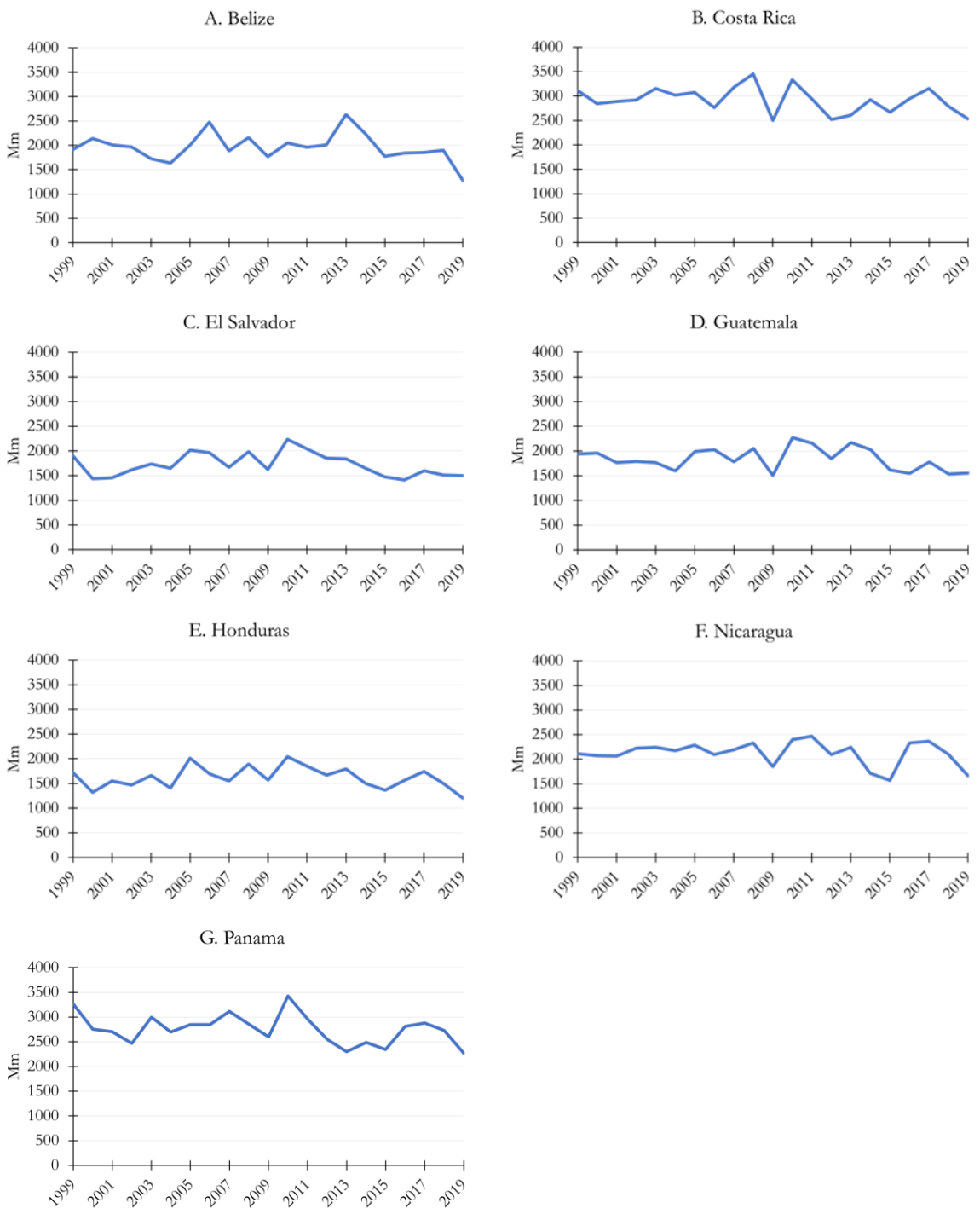

Figure A4. Central America mean precipitation trends from 1999 to 2019.

Table A2.

El Cajon Dam, Honduras Zonal Statistics

Total Precipitation for El Cajón Dam (Honduras)	
Watershed Area:	21,963 km^2
Watershed Precipitation: Hurricane Eta	649 mm
Watershed Precipitation: Hurricane Iota	430 mm
Total Watershed Precipitation: Hurricane Eta & Iota	1079 mm
Total Precipitation: Hurricane Eta & Iota	1451 mm
Percent of Total Precipitation:	74%